NIH Public Access
Author Manuscript
Arterioscler Thromb Vasc Biol. Author manuscript; available in PMC 2010 July 1.

Published in final edited form as:
Arterioscler Thromb Vasc Biol. 2009 July ; 29(7): 1009–1016. doi:10.1161/ATVBAHA.108.165563.

Inflammation Imaging in Atherosclerosis

James H.F. Rudd,
Division of Cardiovascular Medicine, Cambridge University, UK

Fabien Hyafil, and
Department of Cardiology and Nuclear Medicine, Bichat Hospital, Assistance Publique-Hopitaux de Paris and Institut National de la Santé et de la Recherche Medicalé U698, Paris, France

Zahi A. Fayad
Translational and Molecular Imaging Institute, Mount Sinai School of Medicine, New York, New York

Abstract

Inflammation is important at many stages of atherosclerotic plaque development. We highlight several imaging modalities that can quantify the degree of plaque inflammation noninvasively. Imaging of this type might allow testing of novel antiatherosclerosis drugs, identification of patients at risk of plaque rupture, and deeper insight into the biology of the disease. The imaging modalities are discussed in relation to their potential use in these areas.

Keywords

pathophysiology; imaging; computed tomography and magnetic resonance imaging; nuclear cardiology and positron-emission tomography; cardiovascular imaging agents/techniques

Atherosclerosis and its complications will cost around 400 billion dollars of U.S. healthcare spending in 2009.[1] The disease, which has origins in childhood, is responsible for the majority of heart attacks, strokes, and peripheral vascular disease.

Inflammation is involved at many stages of atherosclerosis. Firstly, endothelial cells in early atherosclerosis begin to express molecules on their luminal surface in response to the presence of lipid in the vessel wall. These molecules are of the selectin (P- and E-) and adhesion classes. Once inside the vessel wall, lipid (mainly as low density lipoprotein) is targeted for oxidation and ingestion by inflammatory cells. Recruitment of these cells, predominantly monocytes and T cells, is facilitated as they become slowed and bound by the expressed endothelial adhesion molecules. Macrophages attempt to clear subendothelial lipid from the vessel wall, but in so doing they set up an inflammatory cycle. They release proinflammatory cytokines including interleukin-1, monocyte chemotactic protein-1, and tumor necrosis factor-α. Macrophages may also secrete enzymes capable of directly digesting the fibrous cap of the plaque, including several members of the matrix metalloproteinase (MMP) family. Plaque macrophages have a high rate of apoptosis and along with the accumulated lipid they constitute the “lipid core” of the plaque. A balance is established between the proinflammatory actions of macrophages and infiltrating lymphocytes and the protective layer of smooth muscle cells separating the lipid

Correspondence to Dr. James H.F. Rudd, Division of Cardiovascular Medicine, Cambridge University, UK, jhfr2@cam.ac.uk or Professor Zahi A. Fayad, Translational and Molecular Imaging Institute, Mount Sinai School of Medicine, One Gustave L. Levy Place, New York, NY 10029, Zahi.fayad@maam.edu.
J.H.F.R. and F.H. contributed equally to this review.

Disclosures: None.

NIH-PA Author Manuscript
NIH-PA Author Manuscript
NIH-PA Author Manuscript

NIH-PA Author Manuscript

NIH-PA Author Manuscript

NIH-PA Author Manuscript

core from the vessel lumen. Where the degree of inflammation is sufficient, the fibrous cap can rupture, exposing the thrombogenic lipid core to the bloodstream. This may cause a local arterial thrombosis from which clinical events such as myocardial infarction can result. Recent interest has also focused on the vasovasorum in atherosclerosis. It constitutes a network of blood vessels that supply the plaque with nutrients, but can also act as a portal for further inflammatory cell entry.[2]

Inflammation within the plaque is favored by the presence of vascular risk factors,[3] and logically, can be reduced by risk factor control and appropriate drug therapy.[4] Besides inflammation, there are other plaque phenotypes that are associated with an increased risk of plaque rupture, such as the presence of a thin fibrous cap, a large lipid core, and outward remodeling of the artery wall.[5]

Patients with acute ischemic events usually harbor multiple ruptured atherosclerotic plaques.[6,7] A useful approach to imaging is thus likely to be noninvasive interrogation of several vascular beds. Quantifying plaque inflammation may be valuable for several reasons. If prospective outcome trials show a correlation between plaque inflammation and clinical events then risk prediction algorithms might be improved. Such studies are already underway (see http://www.hrpinitiative.com - due to report in 2011). A second role for inflammation imaging is to allow noninvasive testing of novel drugs. Studies of this type have already been reported.[8,9]

Several noninvasive modalities that can measure different aspects of inflammation are described. The merits and drawbacks of each will be assessed in relation to the pathobiology of atherosclerosis.

Nuclear Imaging

Noninvasive quantification of inflammation can be performed with both of the nuclear imaging techniques - SPECT (single photon emission computed tomography) and PET (positron emission tomography). Both modalities require the use of ionizing radiation. A radioactive tracer is administered intravenously and allowed to circulate within the body. This allows time for the tracer to accumulate at the site of interest, and importantly, time for blood levels to become sufficiently low to generate a favorable target to background signal. Both SPECT and PET have sensitivities for the detection of molecular targets within the picomolar range, translating into the ability to use small doses of contrast agent compared to MRI and computed tomography (CT). Nuclear imaging sensitivities compare favorably with both MRI and especially CT, which have sensitivities up to a trillion times lower (Figure 1). The superior spatial resolution of PET (3 to 4 mm) makes it more attractive than SPECT (10 to 15 mm). However, the resolution of both methods is significantly less than that achieved by either MRI or CT. The high sensitivity of nuclear methods coupled with the favorable resolution of CT and MRI is the driver behind hybrid imaging systems such as PET/CT and PET/MR that are now becoming available.

SPECT

SPECT imaging can image MMP activation and fibrous cap degradation - a principal mechanism of plaque rupture. Different strategies have been used to achieve this. The most successful has been using radiolabeled inhibitors of the activated MMP enzymes. This approach was used by Schafers to image MMP activity in atherosclerotic mice.[10] SPECT imaging of the inhibitor HO-CGS 27023A revealed heavy uptake within plaque and was confirmed by autoradiography, where radiotracer accumulation was almost 3 times greater in the affected plaque compared to the unaffected artery. An MMP inhibitor with a fluorine 18 (18F) PET label[11] to take advantage of the higher spatial resolution of PET has now been

NIH-PA Author Manuscript

NIH-PA Author Manuscript

NIH-PA Author Manuscript

developed. Optical and near-infrared approaches for imaging proteolytic activity have also recently been described.[12,13] These have used a quenched form of the imaging sensor, which is activated by the target enzyme itself, greatly enhancing specificity for activated MMP. Further description of this approach is outside the scope of this work, but the reader is pointed to recent reviews addressing intravascular and optical approaches for atheroma imaging[14–16] (see also Jaffer et al in this series).

Kircher et al used combined SPECT and CT imaging to track the recruitment of indium-labeled monocytes to plaque in atherosclerotic mice, an early stage of plaque development.[17] They showed that after 5 days monocytes had been incorporated into the plaque. Additionally, monocyte accumulation was slowed by statin treatment. T lymphocytes are also present in plaque, and were targeted for imaging by SPECT in patients awaiting carotid endarterectomy. Culprit lesions were selectively visualized by ^{99}Tc-labeled interleukin 2 scintigraphy, and a significant reduction in tracer uptake occurred after 3 months of statin therapy.[18]

PET

PET imaging with 18-F fluorodeoxyglucose (FDG) is the gold standard technique for monitoring the response of tumors to therapy and for the detection of metastatic disease. Arterial FDG uptake was first noted in the aorta of patients undergoing PET imaging for cancer.[19] It was soon appreciated that the degree of FDG uptake increased with age[20] and was higher in those with cardiovascular risk factors.[21–23]

The basis for FDG uptake into the arterial wall is likely attributable to accumulation within plaque macrophages. Supporting evidence comes from cell culture work, where both leukocytes and macrophages demonstrate increases in oxidative metabolism and glucose use in response to cellular activating agents, which is accompanied by a dramatic increase in FDG uptake.[24,25]

In the first prospective study of atherosclerosis imaging with FDG PET, patients with transient ischemic attack (TIA) were scanned shortly after symptom onset. PET revealed that symptomatic carotid plaque accumulated approximately 30% more FDG compared to the asymptomatic artery.[26] FDG PET imaging can also quantify inflammation within the aorta[27,28] and vertebral arteries,[29] where it is possible to differentiate carotid artery from vertebral FDG uptake in patients with posterior circulation stroke syndrome. Uptake in patients with peripheral artery disease is also feasible.[30,31]

In parallel with these proof of principal studies, strong relationships have been documented between the degree of arterial FDG uptake and the density of macrophages determined histologically in both animal models of atherosclerosis[32–34] and in patients with carotid disease.[35]

As well as a marker of inflammation, there are preliminary reports that arterial FDG uptake may also predict plaque rupture and clinical events. In a rabbit model of atherosclerosis, plaque rupture was promoted by venom injection. Only those aortic plaques with the highest preinjection FDG uptake progressed to rupture and thrombosis.[36] In another study involving more than 2000 cancer patients, investigators identified those with (n=45) and without (n=56) arterial FDG uptake on PET scans. Patients with the highest FDG uptake were more likely to have previously suffered a vascular event, or to experience one in the 6 months after imaging.[37]

The short-term interscan reproducibility of FDG PET imaging for atherosclerosis is excellent in the carotid, aorta, and peripheral arteries.[28,31,38] This is important as a precursor to intervention studies (Figure 2). The first study to investigate whether arterial FDG signal could

NIH-PA Author Manuscript

NIH-PA Author Manuscript

NIH-PA Author Manuscript

be reduced with therapy was conducted in a rabbit atherosclerosis model by Ogawa et al.[39] They demonstrated that PET could highlight reduction in FDG uptake after 3 months' therapy with probucol (a lipid lowering antioxidant agent). More recently, a cohort of 43 cancer patients was imaged with FDG PET before and after 3 months of low-dose statin therapy. Compared to placebo group, there was a significant reduction in carotid artery FDG uptake that paralleled the degree of HDL elevation.[8] Another study[40] examined the effect of risk factor modification on arterial FDG uptake in a group of 60 asymptomatic subjects. Interestingly, after 17 months of dietary and lifestyle modifications, there was a 65% reduction in the number of vascular regions that accumulated FDG. The magnitude of the reduction closely paralleled the rise in HDL seen in the patient group.

One limitation of FDG PET is the relatively nonspecific nature of FDG uptake. Although several histological studies described here have shown that there is a strong correlation between FDG uptake and macrophage content of plaque, it is also known that FDG can accumulate within other cells that are involved in the initiation and pathogenesis of atherosclerosis including endothelial cells[41] and lymphocytes.[42] Tracers more specific than FDG for macrophages, including ligands for the peripheral benzodiazepine receptor such as PK11195 and PBR28,[43,44] have shown early promise in this respect.

Other limitations of PET include errors related to the partial volume effect. This occurs when imaging objects smaller than the spatial resolution of PET (3 to 4 mm). The result can be inaccurate quantification of the FDG signal. Partial volume errors can be overcome by using high-resolution MR imaging,[38] where the exact volume of each tissue element within the PET field is determined and used to correct the observed FDG uptake value. The recent introduction of combined PET/MRI scanners will accelerate this effort.[45] Finally, coronary artery imaging presents special problems: cardiac and respiratory movement, myocardial FDG uptake, and the small size (3 to 4 mm) of the coronary arteries. Suppression of myocardial FDG uptake might be possible using a high-fat diet with beta blockade and could be a promising approach.[46]

MRI

MRI allows high-resolution imaging of the arterial wall without ionizing radiation. Spatial resolutions of 250 μm are possible for aorta[47] and carotid plaque.[48] MRI can image the extent of atherosclerosis[49] and can monitor the efficacy of antiatherosclerotic treatments.[50] In addition, elements of the mature atherosclerotic plaque (fibrous cap, lipid core, hemorrhage) can be identified using MRI.[51,52]

However, imaging inflammation within atherosclerotic plaque using MRI requires the injection of a contrast agent. There are two types, paramagnetic and superparamagnetic, that differ in their structure and effect on signal intensity.

Imaging Inflammation Using Paramagnetic Contrast Agents

Paramagnetic contrast agents are composed of lanthanide metals such as gadolinium. They enhance the longitudinal magnetization (T1) of nearby water protons resulting in a positive signal on the MR image.

One approach for evaluating inflammatory activity in plaque by MR is to measure the degree of plaque neovascularization -a phenomenon closely aligned with inflammation. It is believed that inflammatory cells use these vessels as entry portals into the plaque.[53] The technique works by intravenous administration of low-molecular-weight gadolinium chelates and is known as dynamic-contrast enhanced MRI (DCE-MRI). DCE-MRI can estimate both neovessel density and permeability in plaque with high spatial and temporal resolution. The concept was

NIH-PA Author Manuscript

NIH-PA Author Manuscript

NIH-PA Author Manuscript

pioneered in oncology, but preliminary studies in atherosclerotic plaques of rabbits[54] and in human carotid plaques[56] show strong correlations between permeability of neovessels measured with DCE-MRI and histological density of macrophages. Although giving only an indirect evaluation of inflammatory activity in atherosclerotic plaques, DCE-MRI offers the advantage of using a readily available FDA-approved MR contrast agent. It also has favorable reproducibility measures.[55]

Analogous to nuclear and CT imaging, MR contrast agents targeted against molecules involved in inflammation have been developed. Molecular imaging with MRI is challenging because contrast agents must reach micromolar concentrations in tissues to be detectable. For example, P947 is composed of a peptide that specifically binds to MMP, linked covalently to a molecule of gadolinium chelate.[56] One hour after injection of P947, a significantly stronger enhancement was detected with MRI in MMP-rich atherosclerotic plaque of atherosclerotic mice as compared to the aortic wall of wild-type mice (95% versus 10%, respectively). The major advantage of this type of contrast agent is its low molecular weight. This means rapid diffusion into the plaque and the ability to detect specific binding early after injection.

For greater signal amplification, specific peptides or antibodies can be attached to lipid-based "nanoparticles" (such as liposomes, micelles, and lipoproteins) containing a high payload of gadolinium.[57] For example, immunomicelles composed of monoclonal antibodies against the macrophage scavenger receptor (MSR) bound covalently to micelles, each containing around 5900 molecules of gadolinium (MSR-immunomicelles).[58] MSR are strongly expressed by foam cells present in atherosclerotic plaque. When tested in an animal model of atherosclerosis, MSR-immunomicelles increased the signal intensity of atherosclerotic aortas of atherosclerotic mice 24 hours after injection by nearly 80% (Figure 3). In addition, a strong correlation was demonstrated between the intensity of signal enhancement and macrophage content of corresponding histological sections. The same technique has also been used to image oxidized LDL in plaques with MR.[59] Using biomimicry and lipoproteins such as high-density lipoprotein (HDL), a multimodal molecular imaging probe for macrophages has been demonstrated to be very flexible.[60,61] As well as being used for imaging, lipid-based nanoparticles can also be loaded with drugs. For example, nanoparticles targeting alphaV-beta3 integrins expressed on immature endothelial cells have been used to deliver angiostatic drugs to plaque.[62,63]

Imaging Inflammation Using Superparamagnetic Contrast Agents

In contrast to paramagnetic contrast agents that cause an MR signal gain ("positive" contrast), superparamagnetic contrast agents shorten the transverse magnetization (T2*) and induce MR signal loss on T2*-weighted sequences ("negative" contrast). These agents are based on iron oxide particles and can be classified according to particle size. Microparticles of iron oxide (MPIO) are largest, followed by superparamagnetic iron oxides (SPIO), and finally ultrasmall superparamagnetic iron oxides (USPIO). This type of contrast agent is more fully described in another review article in this issue of the Journal (Tang et al).

MPIO are large iron oxide nanoparticles (0.9 to 4.5 μm). Their high iron payload means stronger MR contrast effects than smaller particles such as USPIO. However, the large size of these particles means that they only distribute in the intravascular space and do not enter the plaque. These particles are therefore well suited to evaluate the expression of adhesion molecules on activated endothelial cells. Recently, MPIO were conjugated to monoclonal antibodies against vascular cell adhesion molecule-1 (VCAM-1) and P-selectin. Dual conjugation of MPIO to antibodies against both molecules led to a stronger signal in the aortic root of atherosclerotic mice (detected with ex vivo MRI) than targeting against either VCAM-1 or P-selectin alone.[64]

NIH-PA Author Manuscript

NIH-PA Author Manuscript

NIH-PA Author Manuscript

SPIO and USPIO are composed of an iron oxide core and a coating material to stabilize the core and prevent aggregation. The smaller sizes of SPIO (50 to 300 nm) and USPIO (15 to 30 nm) allow these particles to enter atherosclerotic plaques. Even though both classes of particles are phagocytosized by macrophages in vitro, the mechanism of their uptake differs. The phagocytosis of SPIOs such as ferumoxide is mediated by scavenger receptors[65] and dependent on macrophage activation status,[66] whereas the mechanism of USPIO uptake in macrophages has not been fully described. SPIO accumulation in atherosclerotic plaques of mice has been demonstrated in vivo.[67] In addition, the number of lesional macrophages containing iron particles strongly increased after injection of proinflammatory cytokines. However, SPIO are rapidly cleared from blood by reticulo-endothelial cells which limits their diffusion in atherosclerotic plaques. In contrast, the small size (15 to 30 nm) and dextran coating of the USPIO ferumoxtran lengthen its half life in the bloodstream and favor its phagocytosis by plaque macrophages.[68]

Experimental studies (Figure 4) confirmed that iron oxide particles accumulated in macrophages of atherosclerotic plaques after intravenous injection of ferumoxtran.[69,70] Interestingly, in the aortic wall of angiotensin2-infused atherosclerotic mice, the intensity of ferumoxtran phagocytosis rather than macrophage density decreased under treatment with a p38 MAPK inhibitor.[71]

In human MR studies with USPIO agents, strong signal losses were detected in carotid plaques correlating with accumulation of iron oxide particles in macrophages.[72,73] The effects of high-dose (80 mg) versus low-dose of atorvastatin on macrophage activity in carotid atherosclerotic plaques was investigated with serial ferumoxtran-enhanced MRI. Preliminary results indicate that high dose statin induced a stronger decrease of ferumoxtran uptake in plaques assessed by MRI after 12 weeks of treatment compared with low-dose statin (See Tang et al in this series). Current limitations of ferumoxtran-enhanced MRI are the 36-hour delay after injection before imaging[74] and the difficulty discriminating between specific signal losses generated by the accumulation of ferumoxtran and other artifacts on T2*-weighted sequences.[70] Regarding the latter point, the recent development of MR sequences identifying T2*-effects as “positive” signals (ie, signal increase) should allow better detection of ferumoxtran accumulation within plaque.[75,76]

In contrast to the passive targeting of ferumoxtran to plaque macrophages, cross-linked iron oxide (CLIO) nanoparticles formed by a dextran coating that allows for the binding of monoclonal antibodies or peptides on its surface have been developed for molecular imaging. For example, the contrast agent VINP-28 binds with a high affinity to VCAM-1.[77] After injection of VINP-28, stronger signal losses were detected in the aortic root of atherosclerotic mice compared to statin-treated mice. In addition, VINP-28 colocalized with VCAM-1 expressing cells such as activated endothelial cells, macrophages, and smooth muscle cells on histological sections of atherosclerotic plaques. Similar to gadolinium-containing micelles, CLIO nanoparticles can also be conjugated to fluorescent, infrared, or radioactive probes. The same researchers tested CLIO particles labeled with a PET radiotracer (^{64}Cu) and a fluorophore in atherosclerotic mice. Peak PET activities 24 hours after intravenous injection of these nanoparticles were located in atherosclerotic plaques of apoE mice and correlated with the presence of signal voids detected by MRI. In addition, fluorescence microscopy confirmed the predominant accumulation of these nanoparticles in macrophages of atherosclerotic plaques.[78] Therapeutic approaches are also emerging based on iron oxide nanoparticles. For example, CLIO nanoparticles conjugated to porphirinic photosensitizers[79] accumulated in macrophages and induced cell death after sustained exposure to laser illumination.

NIH-PA Author Manuscript

NIH-PA Author Manuscript

NIH-PA Author Manuscript

Computed Tomography

Computed tomography (CT) scanners have evolved from machines that needed about 300 seconds to obtain a single image to multi-detector machines that can simultaneously acquire 256 or more image "slices" in less than 250 ms. In coronary arteries, early limited spatial and temporal resolution meant that the initial focus was on quantifying calcium deposits within plaque, without injection of contrast agent, yielding a "calcium score." Calcium scores correlate well with the extent of atherosclerosis and have prognostic value.[80,81] However, noncalcified plaques are common, and in patients with acute coronary syndromes seem to be the most prone to rupture.[82]

The current focus is therefore to determine the presence of noncalcified plaque. This effort has been accelerated by several developments. These include great increases in spatial and temporal resolution, along with the introduction of multi-detector CT machines. Currently, CT can identify important features of high-risk atherosclerotic plaque in coronary arteries, such as a speckled pattern of calcification, the presence of a lipid core, and an outward remodeling of the arterial wall.[82–85] Additionally, there is increasing evidence that any degree of coronary atherosclerosis on a CT coronary angiogram confers an adverse prognosis,[86–89] as was shown to be the case many decades ago for x-ray coronary artery imaging.[90,91]

However, inflammatory cells in atherosclerotic plaques cannot be measured using conventional CT contrast agents. Novel agents have been developed for this purpose.[92] For example, N1177 consists of iodinated nanoparticles dispersed with surfactant (mean diameter: 260 nm). A strong increase in plaque density was detected by CT in macrophage-rich atherosclerotic plaques two hours after intravenous injection of N1177 (Figure 5). On corresponding sections of atherosclerotic plaques, iodine nanoparticles were identified in the lysosomes of macrophages with electron microscopy.

CT contrast agents based on electron dense atoms such as bismuth[93] or gold have also been synthesized. Gold nanoparticles incorporated into HDL were detected ex vivo in the aorta of atherosclerotic mice with micro-CT and colocalized with lesional macrophages on histology.[61]

Current limitations of CT include the need for relatively high concentrations of contrast agent to be present at the site of interest (compared with nuclear techniques), and the possible toxicity issues associated with such high doses.

In the future, the use of highly efficient flat-panel detectors[94] will facilitate significant radiation dose reductions. In addition, dual-energy beam technology,[95,96] based on simultaneous CT acquisitions using two beams at different energy levels, should help to improve the sensitivity for contrast agent detection.

Conclusions

We have described several imaging modalities that can detect inflammation in atherosclerotic plaques. However, none of these imaging techniques offers both high spatial resolution and sensitivity. Integrated systems that combine an imaging modality with high spatial resolution (MRI or CT) with one with high sensitivity (PET or SPECT) should help to overcome these limitations.

Some of the imaging techniques such as FDG-PET, DCE MRI, and USPIO-enhanced MRI are close to the clinical arena. Ongoing prospective trials will determine the place of imaging inflammation in predicting clinical events.

NIH-PA Author Manuscript

NIH-PA Author Manuscript

NIH-PA Author Manuscript

Finally, molecular imaging has already spurred the development of platforms that can transport contrast moieties to specific biological targets in atherosclerotic plaque. In the future, these platforms could also simultaneously permit delivery of therapeutic agents to plaques with minimal systemic toxicity - “theranostics.”

Acknowledgments

Sources of Funding: Dr Rudd is funded by the British Heart Foundation. Work described in this review was part-funded by the NIHR Cambridge Biomedical Research Centre. Dr Hyafil is supported by grants from the Federation Française de Cardiologie. Partial funding was provided to Dr Fayad by NIH/NHLBI R01 HL071021 and R01 HL078667.

References

1. Rosamond W, Flegal K, Friday G, Furie K, Go A, Greenlund K, Haase N, Ho M, Howard V, Kissela B, Kittner S, Lloyd-Jones D, McDermott M, Meigs J, Moy C, Nichol G, O'Donnell CJ, Roger V, Rumsfeld J, Sorlie P, Steinberger J, Thom T, Wasserthiel-Smoller S, Hong Y, for the American Heart Association Statistics Committee and Stroke Statistics Subcommittee. Heart Disease and Stroke Statistics–2007 Update: A Report From the American Heart Association Statistics Committee and Stroke Statistics Subcommittee. Circulation 2007;115:e69–e171. [PubMed: 17194875]
2. Virmani R, Burke AP, Farb A, Kolodgie FD. Pathology of the vulnerable plaque. J Am Coll Cardiol 2006;47:C13–C18. [PubMed: 16631505]
3. Burke AP, Farb A, Malcom GT, Liang YH, Smialek J, Virmani R. Coronary risk factors and plaque morphology in men with coronary disease who died suddenly. N Engl J Med 1997;336:1276–1282. [PubMed: 9113930]
4. Crisby M, Nordin-Fredriksson G, Shah PK, Yano J, Zhu J, Nilsson J. Pravastatin treatment increases collagen content and decreases lipid content, inflammation, metalloproteinases, and cell death in human carotid plaques: implications for plaque stabilization. Circulation 2001;103:926–933. [PubMed: 11181465]
5. Naghavi M, Falk E, Hecht HS, Jamieson MJ, Kaul S, Berman DS, Fayad ZA, Budoff MJ, Rumberger J, Naqvi TZ, Shaw LJ, Faergeman O, Cohn J, Bahr R, Koenig W, Demirovic J, Arking D, Herrera VL, Badimon JJ, Goldstein JA, Rudy Y, Airaksinen J, Schwartz RS, Riley WA, Mendes RA, Douglas P, Shah PK, Force ST. From vulnerable plaque to vulnerable patient–Part III: Executive summary of the Screening for Heart Attack Prevention and Education (SHAPE) Task Force report. The Am J Cardiol 2006;98:2H–15H.
6. Rioufol G, Finet G, Ginon I, Andre-Fouet X, Rossi R, Vialle E, Desjoyaux E, Convert G, Huret JF, Tabib A. Multiple atherosclerotic plaque rupture in acute coronary syndrome: a three-vessel intravascular ultrasound study. Circulation 2002;106:804–808. [PubMed: 12176951]
7. Mauriello A, Sangiorgi G, Fratoni S, Palmieri G, Bonanno E, Anemona L, Schwartz RS, Spagnoli LG. Diffuse and active inflammation occurs in both vulnerable and stable plaques of the entire coronary tree: a histopathologic study of patients dying of acute myocardial infarction. J Am Coll Cardiol 2005;45:1585–1593. [PubMed: 15893171]
8. Tahara N, Kai H, Ishibashi M, Nakaura H, Kaida H, Baba K, Hayabuchi N, Imaizumi T. Simvastatin attenuates plaque inflammation: evaluation by fluorodeoxyglucose positron emission tomography. J AmCollCardiol 2006;48:1825–1831.
9. Lee SJ, On YK, Lee EJ, Choi JY, Kim BT, Lee KH. Reversal of vascular 18F-FDG uptake with plasma high-density lipoprotein elevation by atherogenic risk reduction. J Nucl Med 2008;49:1277–1282. [PubMed: 18632820]
10. Schafers M, Riemann B, Kopka K, Breyholz HJ, Wagner S, Schafers KP, Law MP, Schober O, Levkau B. Scintigraphic imaging of matrix metalloproteinase activity in the arterial wall in vivo. Circulation 2004;109:2554–2559. [PubMed: 15123523]
11. Breyholz HJ, Wagner S, Levkau B, Schober O, Schafers M, Kopka K. A 18F-radiolabeled analogue of CGS 27023A as a potential agent for assessment of matrix-metalloproteinase activity in vivo. QJ Nucl Med MolImaging 2007;51:24–32.

NIH-PA Author Manuscript

NIH-PA Author Manuscript

NIH-PA Author Manuscript

12. Faust A, Waschkau B, Waldeck J, Höltke C, Breyholz HJ, Wagner S, Kopka K, Heindel W, Schäfers M, Bremer C. Synthesis and evaluation of a novel fluorescent photoprobe for imaging matrix metalloproteinases. Bioconjugate chemistry 2008;19:1001–1008. [PubMed: 18396900]
13. Jaffer FA, Vinegoni C, John MC, Aikawa E, Gold HK, Finn AV, Ntziachristos V, Libby P, Weissleder R. Real-time catheter molecular sensing of inflammation in proteolytically active atherosclerosis. Circulation 2008;118:1802–1809. [PubMed: 18852366]
14. Lindsay AC, Choudhury R. Form to function: current and future roles for atherosclerosis imaging in drug development. Nat Rev Drug Disc 2008;7:517–529.
15. Honda Y, Fitzgerald PJ. Frontiers in intravascular imaging technologies. Circulation 2008;117:2024–2037. [PubMed: 18413510]
16. Langer HF, Haubner R, Pichler BJ, Gawaz M. Radionuclide imaging: a molecular key to the atherosclerotic plaque. J Am Coll Cardiol 2008;52:1–12. [PubMed: 18582628]
17. Kircher MF, Grimm J, Swirski FK, Libby P, Gerszten RE, Allport JR, Weissleder R. Noninvasive in vivo imaging of monocyte trafficking to atherosclerotic lesions. Circulation 2008;117:388–395. [PubMed: 18172031]
18. Annovazzi A, Bonanno E, Arca M, D'alessandria C, Marcoccia A, Spagnoli L, Violi F, Scopinaro F, Toma G, Signore A. 99mTc-interleukin-2 scintigraphy for the in vivo imaging of vulnerable atherosclerotic plaques. Eur J Nucl Med Mol Imaging 2006;33:117–126. [PubMed: 16220305]
19. Yun M, Yeh D, Araujo LI, Jang S, Newberg A, Alavi A. F-18 FDG uptake in the large arteries: a new observation. Clin Nucl Med 2001;26:314–319. [PubMed: 11290891]
20. Yun M, Jang S, Cucchiara A, Newberg AB, Alavi A. 18F FDG uptake in the large arteries: a correlation study with the atherogenic risk factors. Sem Nucl Med 2002;32:70–76.
21. Tatsumi M, Cohade C, Nakamoto Y, Wahl RL. Fluorodeoxyglucose uptake in the aortic wall at PET/CT: possible finding for active atherosclerosis. Radiology 2003;229:831–837. [PubMed: 14593193]
22. Tahara N, Kai H, Yamagishi S, Mizoguchi M, Nakaura H, Ishibashi M, Kaida H, Baba K, Hayabuchi N, Imaizumi T. Vascular inflammation evaluated by [18F]-fluorodeoxyglucose positron emission tomography is associated with the metabolic syndrome. J Am Coll Cardiol 2007;49:1533–1539. [PubMed: 17418291]
23. Tahara N, Kai H, Nakaura H, Mizoguchi M, Ishibashi M, Kaida H, Baba K, Hayabuchi N, Imaizumi T. The prevalence of inflammation in carotid atherosclerosis: analysis with fluorodeoxyglucose-positron emission tomography. Eur Heart J 2007;28:2243–2248. [PubMed: 17681956]
24. Deichen JT, Prante O, Gack M, Schmiedehausen K, Kuwert T. Uptake of [(18)F]fluorodeoxyglucose in human monocyte-macrophages in vitro. EurJ Nucl MedMolImaging 2003;30:267–273.
25. Forstrom LA, Dunn WL, Mullan BP, Hung JC, Lowe VJ, Thorson LM. Biodistribution and dosimetry of [(18)F]fluorodeoxyglucose labelled leukocytes in normal human subjects. Nucl Med Commun 2002;23:721–725. [PubMed: 12124476]
26. Rudd J, Warburton E, Fryer T, Jones H, Clark J, Antoun N, Johnström P, Davenport A, Kirkpatrick P, Arch B, Pickard J, Weissberg P. Imaging atherosclerotic plaque inflammation with [18F]-fluorodeoxyglucose positron emission tomography. Circulation 2002;105:2708–2711. [PubMed: 12057982]
27. Dunphy MP, Freiman A, Larson SM, Strauss HW. Association of Vascular 18F-FDG Uptake with Vascular Calcification. J Nucl Med 2005;46:1278–1284. [PubMed: 16085583]
28. Rudd J, Myers K, Bansilal S, Machac J, Rafique A, Farkouh M, Fuster V, Fayad Z. (18) Fluorodeoxyglucose positron emission tomography imaging of atherosclerotic plaque inflammation is highly reproducible: implications for atherosclerosis therapy trials. J Am Coll Cardiol 2007;50:892–896. [PubMed: 17719477]
29. Davies JR, Rudd JH, Fryer TD, Graves MJ, Clark JC, Kirkpatrick PJ, Gillard JH, Warburton EA, Weissberg PL. Identification of culprit lesions after transient ischemic attack by combined 18F fluorodeoxyglucose positron-emission tomography and high-resolution magnetic resonance imaging. Stroke 2005;36:2642–2647. [PubMed: 16282536]
30. Basu S, Zhuang H, Alavi A. Imaging of lower extremity artery atherosclerosis in diabetic foot: FDG-PET imaging and histopathological correlates. Clin Nucl Med 2007;32:567–568. [PubMed: 17581350]

NIH-PA Author Manuscript

NIH-PA Author Manuscript

NIH-PA Author Manuscript

31. Rudd JH, Myers KS, Bansilal S, Machac J, Pinto CA, Tong C, Rafique A, Hargeaves R, Farkouh M, Fuster V, Fayad ZA. Atherosclerosis inflammation imaging with 18F-FDG PET: carotid, iliac, and femoral uptake reproducibility, quantification methods, and recommendations. J Nucl Med 2008;49:871–878. [PubMed: 18483100]
32. Ogawa M, Ishino S, Mukai T, Asano D, Teramoto N, Watabe H, Kudomi N, Shiomi M, Magata Y, Iida H, Saji H. (18)F-FDG accumulation in atherosclerotic plaques: immunohistochemical and PET imaging study. J Nucl Med 2004;45:1245–1250. [PubMed: 15235073]
33. Tawakol A, Migrino RQ, Hoffmann U, Abbara S, Houser S, Gewirtz H, Muller JE, Brady TJ, Fischman AJ. Noninvasive in vivo measurement of vascular inflammation with F-18 fluorodeoxyglucose positron emission tomography. J Nucl Cardiol 2005;12:294–301. [PubMed: 15944534]
34. Zhang Z, Machac J, Helft G, Worthley SG, Tang C, Zaman AG, Rodriguez OJ, Buchsbaum MS, Fuster V, Badimon JJ. Non-invasive imaging of atherosclerotic plaque macrophage in a rabbit model with F-18 FDG PET: a histopathological correlation. BMC Nucl Med 2006;6:3. [PubMed: 16725052]
35. Tawakol A, Migrino RQ, Bashian GG, Bedri S, Vermylen D, Cury RC, Yates D, LaMuraglia GM, Furie K, Houser S, Gewirtz H, Muller JE, Brady TJ, Fischman AJ. In vivo 18F-fluorodeoxyglucose positron emission tomography imaging provides a noninvasive measure of carotid plaque inflammation in patients. J Am Coll Cardiol 2006;48:1818–1824. [PubMed: 17084256]
36. Aziz K, Berger K, Claycombe K, Huang R, Patel R, Abela GS. Noninvasive detection and localization of vulnerable plaque and arterial thrombosis with computed tomography angiography/positron emission tomography. Circulation 2008;117:2061–2070. [PubMed: 18391115]
37. Paulmier B, Duet M, Khayat R, Pierquet-Ghazzar N, Laissy JP, Maunoury C, Hugonnet F, Sauvaget E, Trinquart L, Faraggi M. Arterial wall uptake of fluorodeoxyglucose on PET imaging in stable cancer disease patients indicates higher risk for cardiovascular events. J Nucl Cardiol 2008;15:209–217. [PubMed: 18371592]
38. Izquierdo-Garcia D, Davies JR, Graves MJ, Rudd JHF, Gillard JH, Weissberg PL, Fryer TD, Warburton EA. Comparison of methods for magnetic resonance-guided [18-f]fluorodeoxyglucose positron emission tomography in human carotid arteries: reproducibility, partial volume correction, and correlation between methods. Stroke 2009;40:86–93. [PubMed: 18927453]
39. Ogawa M, Magata Y, Kato T, Hatano K, Ishino S, Mukai T, Shiomi M, Ito K, Saji H. Application of 18F-FDG PET for monitoring the therapeutic effect of antiinflammatory drugs on stabilization of vulnerable atherosclerotic plaques. J Nucl Med 2006;47:1845–1850. [PubMed: 17079818]
40. Lee JM, Wiesmann F, Shirodaria C, Leeson P, Petersen SE, Francis JM, Jackson CE, Robson MD, Neubauer S, Channon K, Choudhury R. Early changes in arterial structure and function following statin initiation: quantification by magnetic resonance imaging. Atherosclerosis 2008;197:951–958. [PubMed: 17977546]
41. Maschauer S, Prante O, Hoffmann M, Deichen JT, Kuwert T. Characterization of 18F-FDG uptake in human endothelial cells in vitro. J Nucl Med 2004;45:455–460. [PubMed: 15001687]
42. Ishimori T, Saga T, Mamede M, Kobayashi H, Higashi T, Nakamoto Y, Sato N, Konishi J. Increased (18)F-FDG uptake in a model of inflammation: concanavalin A-mediated lymphocyte activation. J Nucl Med 2002;43:658–663. [PubMed: 11994531]
43. Imaizumi M, Briard E, Zoghbi SS, Gourley JP, Hong J, Fujimura Y, Pike VW, Innis RB, Fujita M. Brain and whole-body imaging in nonhuman primates of [11C]PBR28, a promising PET radioligand for peripheral benzodiazepine receptors. NeuroImage 2008;39:1289–1298. [PubMed: 18024084]
44. Fujimura Y, Hwang PM, Trout H Iii, Kozloff L, Imaizumi M, Innis RB, Fujita M. Increased peripheral benzodiazepine receptors in arterial plaque of patients with atherosclerosis: An autoradiographic study with [(3)H]PK 11195. Atherosclerosis. 2008
45. Pichler B, Judenhofer M, Wehrl H. PET/MRI hybrid imaging: devices and initial results. Eur Radiol 2008;18:1077–1086. [PubMed: 18357456]
46. Williams G, Kolodny GM. Suppression of myocardial 18F-FDG uptake by preparing patients with a high-fat, low-carbohydrate diet. AJR Am J Roentgenol 2008;190:W151–W156. [PubMed: 18212199]
47. Yonemura A, Momiyama Y, Fayad ZA, Ayaori M, Ohmori R, Higashi K, Kihara T, Sawada S, Iwamoto N, Ogura M, Taniguchi H, Kusuhara M, Nagata M, Nakamura H, Tamai S, Ohsuzu F. Effect

NIH-PA Author Manuscript

NIH-PA Author Manuscript

NIH-PA Author Manuscript

of lipid-lowering therapy with atorvastatin on atherosclerotic aortic plaques detected by noninvasive magnetic resonance imaging. J Am Coll Cardiol 2005;45:733–742. [PubMed: 15734619]

48. Yuan C, Beach KW, Smith LH Jr, Hatsukami TS. Measurement of atherosclerotic carotid plaque size in vivo using high resolution magnetic resonance imaging. Circulation 1998;98:2666–2671. [PubMed: 9851951]
49. Fayad ZA, Nahar T, Fallon JT, Goldman M, Aguinaldo JG, Badimon JJ, Shinnar M, Chesebro JH, Fuster V. In vivo magnetic resonance evaluation of atherosclerotic plaques in the human thoracic aorta: a comparison with transesophageal echocardiography. Circulation 2000;101:2503–2509. [PubMed: 10831525]
50. Corti R, Fuster V, Fayad ZA, Worthley SG, Helft G, Smith D, Weinberger J, Wentzel J, Mizsei G, Mercuri M, Badimon JJ. Lipid lowering by simvastatin induces regression of human atherosclerotic lesions: two years' follow-up by high-resolution noninvasive magnetic resonance imaging. Circulation 2002;106:2884–2887. [PubMed: 12460866]
51. Fayad ZA, Fuster V. Characterization of atherosclerotic plaques by magnetic resonance imaging. Ann N Y Acad Sci 2000;902:173–186. [PubMed: 10865837]
52. Yuan C, Ferguson MS, Kerwin W, Polissar N, Cai J, Hatsukami TS. Contrast enhanced high resolution MRI for atherosclerotic carotid tissue characterization. Proc Intl Soc Mag Reson Med 2001;9:641.
53. Kerwin W, Hooker A, Spilker M, Vicini P, Ferguson M, Hatsukami T, Yuan C. Quantitative magnetic resonance imaging analysis of neovasculature volume in carotid atherosclerotic plaque. Circulation 2003;107:851–856. [PubMed: 12591755]
54. Calcagno C, Cornily JC, Hyafil F, Rudd JH, Briley-Saebo KC, Mani V, Goldschlager G, Machac J, Fuster V, Fayad ZA. Detection of neovessels in atherosclerotic plaques of rabbits using dynamic contrast enhanced MRI and 18F-FDG PET. Arterioscler Thromb Vasc Biol 2008;28:1311–1317. [PubMed: 18467641]
55. Kerwin WS, Oikawa M, Yuan C, Jarvik GP, Hatsukami TS. MR imaging of adventitial vasa vasorum in carotid atherosclerosis. Magn Reson Med 2008;59:507–514. [PubMed: 18306402]
56. Lancelot E, Amirbekian V, Brigger I, Raynaud JS, Ballet S, David C, Rousseaux O, Le Greneur S, Port M, Lijnen HR, Bruneval P, Michel JB, Ouimet T, Roques B, Amirbekian S, Hyafil F, Vucic E, Aguinaldo JG, Corot C, Fayad ZA. Evaluation of matrix metalloproteinases in atherosclerosis using a novel noninvasive imaging approach. Arterioscler Thromb Vasc Biol 2008;28:425–432. [PubMed: 18258820]
57. Briley-Saebo KC, Mulder WJ, Mani V, Hyafil F, Amirbekian V, Aguinaldo JG, Fisher EA, Fayad ZA. Magnetic resonance imaging of vulnerable atherosclerotic plaques: current imaging strategies and molecular imaging probes. J Magn Reson Imaging 2007;26:460–479. [PubMed: 17729343]
58. Amirbekian V, Lipinski MJ, Briley-Saebo KC, Amirbekian S, Aguinaldo JG, Weinreb DB, Vucic E, Frias JC, Hyafil F, Mani V, Fisher EA, Fayad ZA. Detecting and assessing macrophages in vivo to evaluate atherosclerosis noninvasively using molecular MRI. Proc Natl Acad Sci USA 2007;104:961–966. [PubMed: 17215360]
59. Briley-Saebo KC, Shaw PX, Mulder WJ, Choi SH, Vucic E, Aguinaldo JG, Witztum JL, Fuster V, Tsimikas S, Fayad ZA. Targeted molecular probes for imaging atherosclerotic lesions with magnetic resonance using antibodies that recognize oxidation-specific epitopes. Circulation 2008;117:3206–3215. [PubMed: 18541740]
60. Cormode DP, Briley-Saebo KC, Mulder WJ, Aguinaldo JG, Barazza A, Ma Y, Fisher E, Fayad ZA. An ApoA-I mimetic peptide high-density-lipoprotein-based MRI contrast agent for atherosclerotic plaque composition detection. Small (Weinheim an der Bergstrasse, Germany) 2008;4:1437–1444.
61. Cormode DP, Skajaa T, van Schooneveld MM, Koole R, Jarzyna P, Lobatto ME, Calcagno C, Barazza A, Gordon RE, Zanzonico P, Fisher EA, Fayad ZA, Mulder WJ. Nanocrystal core high-density lipoproteins: a multimodality contrast agent platform. Nano Lett 2008;8:3715–3723. [PubMed: 18939808]
62. Winter PM, Neubauer AM, Caruthers SD, Harris TD, Robertson JD, Williams TA, Schmieder AH, Hu G, Allen JS, Lacy EK, Zhang H, Wickline SA, Lanza GM. Endothelial alpha(v) beta3 integrin-targeted fumagillin nanoparticles inhibit angiogenesis in atherosclerosis. Arterioscler Thromb Vasc Biol 2006;26:2103–2109. [PubMed: 16825592]

NIH-PA Author Manuscript

NIH-PA Author Manuscript

NIH-PA Author Manuscript

63. Mulder WJ, van der Schaft DW, Hautvast PA, Strijkers GJ, Koning GA, Storm G, Mayo KH, Griffioen AW, Nicolay K. Early in vivo assessment of angiostatic therapy efficacy by molecular MRI. Faseb J 2007;21:378–383. [PubMed: 17202248]
64. McAteer MA, Schneider JE, Ali ZA, Warrick N, Bursill CA, von zur Muhlen C, Greaves DR, Neubauer S, Channon KM, Choudhury RP. Magnetic resonance imaging of endothelial adhesion molecules in mouse atherosclerosis using dual-targeted microparticles of iron oxide. Arterioscler Thromb Vasc Biol 2008;28:77–83. [PubMed: 17962629]
65. Raynal I, Prigent P, Peyramaure S, Najid A, Rebuzzi C, Corot C. Macrophage endocytosis of superparamagnetic iron oxide nanoparticles: mechanisms and comparison of ferumoxides and ferumoxtran-10. Invest Radiol 2004;39:56–63. [PubMed: 14701989]
66. von Zur Muhlen C, von Elverfeldt D, Bassler N, Neudorfer I, Steitz B, Petri-Fink A, Hofmann H, Bode C, Peter K. Superparamagnetic iron oxide binding and uptake as imaged by magnetic resonance is mediated by the integrin receptor Mac-1 (CD11b/CD18): implications on imaging of atherosclerotic plaques. Atherosclerosis 2007;193:102–111. [PubMed: 16997307]
67. Litovsky S, Madjid M, Zarrabi A, Casscells SW, Willerson JT, Naghavi M. Superparamagnetic iron oxide-based method for quantifying recruitment of monocytes to mouse atherosclerotic lesions in vivo: enhancement by tissue necrosis factor-alpha, interleukin-1beta, and interferon-gamma. Circulation 2003;107:1545–1549. [PubMed: 12654614]
68. Yancy AD, Olzinski AR, Hu TC, Lenhard SC, Aravindhan K, Gruver SM, Jacobs PM, Willette RN, Jucker BM. Differential uptake of ferumoxtran-10 and ferumoxytol, ultrasmall superparamagnetic iron oxide contrast agents in rabbit: critical determinants of atherosclerotic plaque labeling. J Magn Reson Imaging 2005;21:432–442. [PubMed: 15779033]
69. Ruehm SG, Corot C, Vogt P, Kolb S, Debatin JF. Magnetic resonance imaging of atherosclerotic plaque with ultrasmall superparamagnetic particles of iron oxide in hyperlipidemic rabbits. Circulation 2001;103:415–422. [PubMed: 11157694]
70. Hyafil F, Laissy JP, Mazighi M, Tchetche D, Louedec L, Adle-Biassette H, Chillon S, Henin D, Jacob MP, Letourneur D, Feldman LJ. Ferumoxtran-10-enhanced MRI of the hypercholesterolemic rabbit aorta: relationship between signal loss and macrophage infiltration. Arterioscler Thromb Vasc Biol 2006;26:176–181. [PubMed: 16269663]
71. Morris JB, Olzinski AR, Bernard RE, Aravindhan K, Mirabile RC, Boyce R, Willette RN, Jucker BM. p38 MAPK inhibition reduces aortic ultrasmall superparamagnetic iron oxide uptake in a mouse model of atherosclerosis: MRI assessment. Arterioscler Thromb Vasc Biol 2008;28:265–271. [PubMed: 18162612]
72. Kooi ME, Cappendijk VC, Cleutjens KB, Kessels AG, Kitslaar PJ, Borgers M, Frederik PM, Daemen MJ, van Engelshoven JM. Accumulation of ultrasmall superparamagnetic particles of iron oxide in human atherosclerotic plaques can be detected by in vivo magnetic resonance imaging. Circulation 2003;107:2453–2458. [PubMed: 12719280]
73. Trivedi RA, Mallawarachi C, U-King-Im J, Graves MJ, Horsley J, Goddard MJ, Brown A, Wang L, Kirkpatrick PJ, Brown J, Gillard JH. Identifying inflamed carotid plaques using in vivo USPIO-enhanced MR imaging to label plaque macrophages. Arterioscler Thromb Vasc Biol 2006;26:1601–1606. [PubMed: 16627809]
74. Trivedi RA, UK-I JM, Graves MJ, Cross JJ, Horsley J, Goddard MJ, Skepper JN, Quartey G, Warburton E, Joubert I, Wang L, Kirkpatrick PJ, Brown J, Gillard JH. In vivo detection of macrophages in human carotid atheroma: temporal dependence of ultrasmall superparamagnetic particles of iron oxide-enhanced MRI. Stroke 2004;35:1631–1635. [PubMed: 15166394]
75. Briley-Saebo KC, Mani V, Hyafil F, Cornily JC, Fayad ZA. Fractionated Feridex and positive contrast: in vivo MR imaging of atherosclerosis. Magn Reson Med 2008;59:721–730. [PubMed: 18383304]
76. Korosoglou G, Weiss RG, Kedziorek DA, Walczak P, Gilson WD, Schar M, Sosnovik DE, Kraitchman DL, Boston RC, Bulte JW, Weissleder R, Stuber M. Noninvasive detection of macrophage-rich atherosclerotic plaque in hyperlipidemic rabbits using “positive contrast” magnetic resonance imaging. J Am Coll Cardiol 2008;52:483–491. [PubMed: 18672170]
77. Nahrendorf M, Jaffer FA, Kelly KA, Sosnovik DE, Aikawa E, Libby P, Weissleder R. Noninvasive vascular cell adhesion molecule-1 imaging identifies inflammatory activation of cells in atherosclerosis. Circulation 2006;114:1504–1511. [PubMed: 17000904]

NIH-PA Author Manuscript

NIH-PA Author Manuscript

NIH-PA Author Manuscript

78. Nahrendorf M, Zhang H, Hembrador S, Panizzi P, Sosnovik DE, Aikawa E, Libby P, Swirski FK, Weissleder R. Nanoparticle PET-CT imaging of macrophages in inflammatory atherosclerosis. Circulation 2008;117:379–387. [PubMed: 18158358]
79. McCarthy JR, Weissleder R. Multifunctional magnetic nanoparticles for targeted imaging and therapy. Adv Drug Deliv Rev 2008;60:1241–1251. [PubMed: 18508157]
80. Greenland P, LaBree L, Azen SP, Doherty TM, Detrano RC. Coronary Artery Calcium Score Combined With Framingham Score for Risk Prediction in Asymptomatic Individuals. JAMA 2004;291:210–215. [PubMed: 14722147]
81. Arad Y, Goodman KJ, Roth M, Newstein D, Guerci AD. Coronary calcification, coronary disease risk factors, C-reactive protein, and atherosclerotic cardiovascular disease events: the St. Francis Heart Study. J Am Coll Cardiol 2005;46:158–165. [PubMed: 15992651]
82. Motoyama S, Kondo T, Sarai M, Sugiura A, Harigaya H, Sato T, Inoue K, Okumura M, Ishii J, Anno H, Virmani R, Ozaki Y, Hishida H, Narula J. Multislice computed tomographic characteristics of coronary lesions in acute coronary syndromes. J Am Coll Cardiol 2007;50:319–326. [PubMed: 17659199]
83. Achenbach S, Moselewski F, Ropers D, Ferencik M, Hoffmann U, MacNeill B, Pohle K, Baum U, Anders K, Jang IK, Daniel WG, Brady TJ. Detection of calcified and noncalcified coronary atherosclerotic plaque by contrast-enhanced, submillimeter multidetector spiral computed tomography: a segment-based comparison with intravascular ultrasound. Circulation 2004;109:14–17. [PubMed: 14691045]
84. Leber AW, Knez A, von Ziegler F, Becker A, Nikolaou K, Paul S, Wintersperger B, Reiser M, Becker CR, Steinbeck G, Boekstegers P. Quantification of obstructive and nonobstructive coronary lesions by 64-slice computed tomography: a comparative study with quantitative coronary angiography and intravascular ultrasound. J Am Coll Cardiol 2005;46:147–154. [PubMed: 15992649]
85. Achenbach S, Ropers D, Hoffmann U, MacNeill B, Baum U, Pohle K, Brady TJ, Pomerantsev E, Ludwig J, Flachskampf FA, Wicky S, Jang IK, Daniel WG. Assessment of coronary remodeling in stenotic and nonstenotic coronary atherosclerotic lesions by multidetector spiral computed tomography. J Am Coll Cardiol 2004;43:842–847. [PubMed: 14998627]
86. Leber A, von Ziegler F, Becker A, Becker C, Reiser M, Steinbeck G, Knez A, Boekstegers P. Characteristics of coronary plaques before angiographic progression determined by Multi-Slice CT. Int J Cardiovasc Imaging 2008;24:423–428. [PubMed: 17990073]
87. Pundziute G, Schuijf JD, Jukema JW, Boersma E, de Roos A, van der Wall EE, Bax JJ. Prognostic value of multislice computed tomography coronary angiography in patients with known or suspected coronary artery disease. J Am Coll Cardiol 2007;49:62–70. [PubMed: 17207724]
88. Min JK, Shaw LJ, Devereux RB, Okin PM, Weinsaft JW, Russo DJ, Lippolis NJ, Berman DS, Callister TQ. Prognostic Value of Multidetector Coronary Computed Tomographic Angiography for Prediction of All-Cause Mortality. J Am Coll Cardiol 2007;50:1161–1170. [PubMed: 17868808]
89. Matsumoto N, Sato Y, Yoda S, Nakano Y, Kunimasa T, Matsuo S, Komatsu S, Saito S, Hirayama A. Prognostic value of non-obstructive CT low-dense coronary artery plaques detected by multislice computed tomography. Circ J 2007;71:1898–1903. [PubMed: 18037743]
90. Mark DB, Nelson CL, Califf RM, Harrell FE Jr, Lee KL, Jones RH, Fortin DF, Stack RS, Glower DD, Smith LR, et al. Continuing evolution of therapy for coronary artery disease. Initial results from the era of coronary angioplasty. Circulation 1994;89:2015–2025. [PubMed: 8181125]
91. Califf RM, Harrell FE Jr, Lee KL, Rankin JS, Hlatky MA, Mark DB, Jones RH, Muhlbaier LH, Oldham HN Jr, Pryor DB. The evolution of medical and surgical therapy for coronary artery disease. A 15-year perspective. JAMA 1989;261:2077–2086. [PubMed: 2784512]
92. Hyafil F, Cornily JC, Feig JE, Gordon R, Vucic E, Amirbekian V, Fisher EA, Fuster V, Feldman LJ, Fayad ZA. Noninvasive detection of macrophages using a nanoparticulate contrast agent for computed tomography. Nat Med 2007;13:636–641. [PubMed: 17417649]
93. Rabin O, Manuel Perez J, Grimm J, Wojtkiewicz G, Weissleder R. An X-ray computed tomography imaging agent based on long-circulating bismuth sulphide nanoparticles. Nat Mater 2006;5:118–122. [PubMed: 16444262]

NIH-PA Author Manuscript

NIH-PA Author Manuscript

NIH-PA Author Manuscript

94. Gupta R, Grasruck M, Suess C, Bartling SH, Schmidt B, Stierstorfer K, Popescu S, Brady T, Flohr T. Ultra-high resolution flat-panel volume CT: fundamental principles, design architecture, and system characterization. Eur Radiol 2006;16:1191–1205. [PubMed: 16528556]

95. Flohr TG, McCollough CH, Bruder H, Petersilka M, Gruber K, Suss C, Grasruck M, Stierstorfer K, Krauss B, Raupach R, Primak AN, Kuttner A, Achenbach S, Becker C, Kopp A, Ohnesorge BM. First performance evaluation of a dual-source CT (DSCT) system. Eur Radiol 2006;16:256–268. [PubMed: 16341833]

96. Boll DT, Hoffmann MH, Huber N, Bossert AS, Aschoff AJ, Fleiter TR. Spectral coronary multidetector computed tomography angiography: dual benefit by facilitating plaque characterization and enhancing lumen depiction. J Comput Assist Tomogr 2006;30:804–811. [PubMed: 16954934]

NIH-PA Author Manuscript

NIH-PA Author Manuscript

NIH-PA Author Manuscript

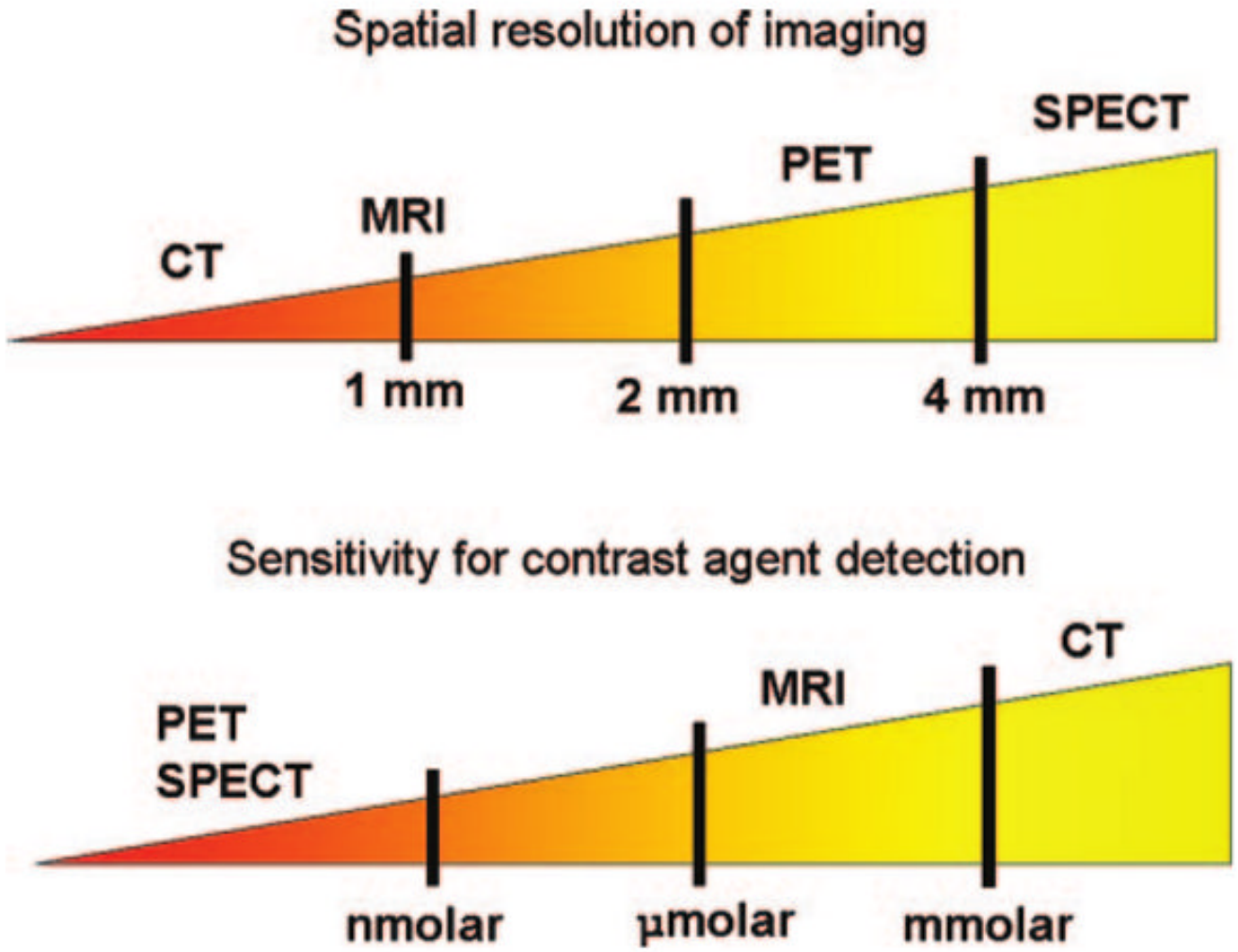

Figure 1.
Illustration of the relative spatial resolution of common imaging techniques (top), along with their sensitivity values (bottom).

NIH-PA Author Manuscript
NIH-PA Author Manuscript
NIH-PA Author Manuscript

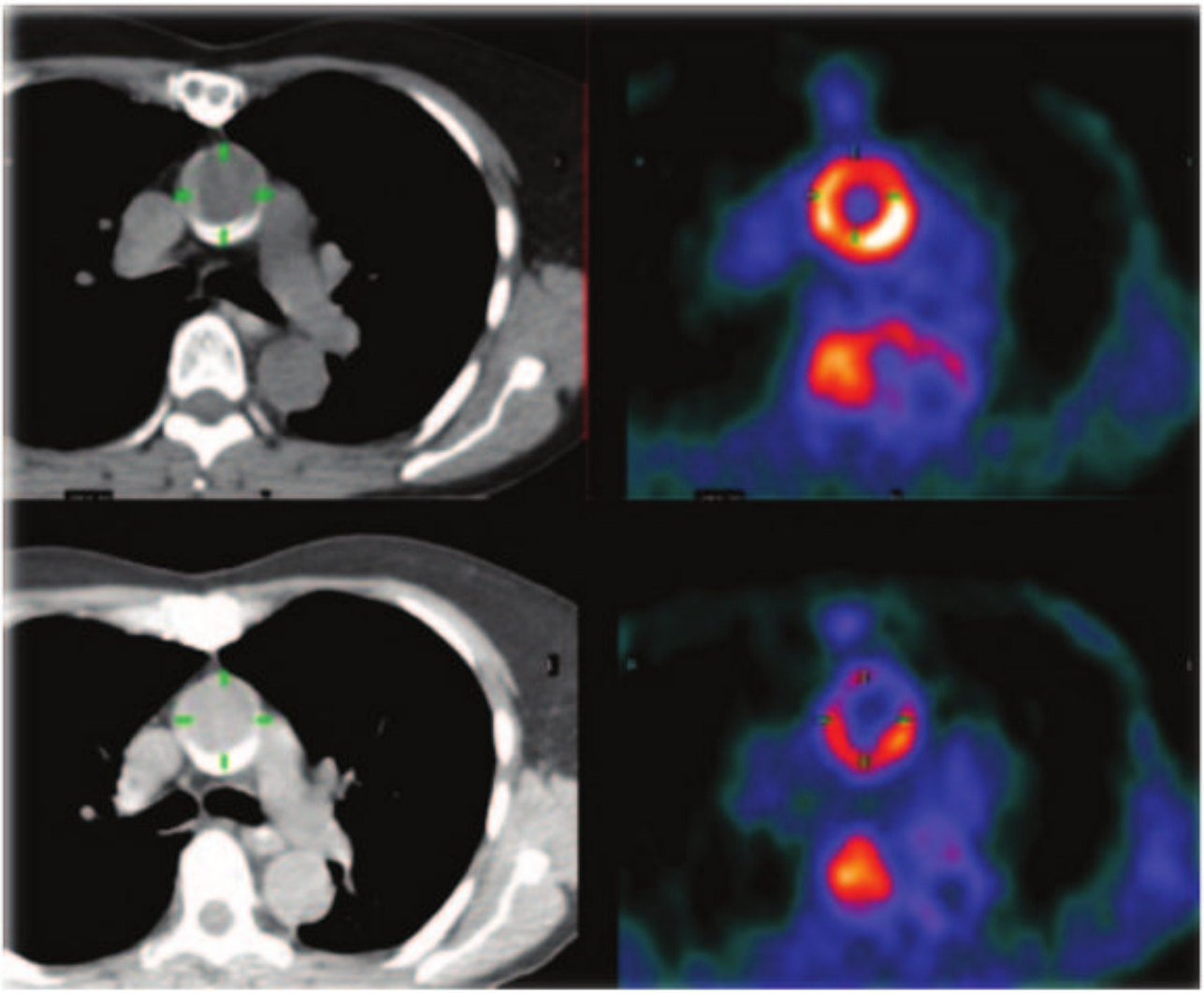

Figure 2.
PET/CT image of aorta before (top) and during (bottom) antiatherosclerosis therapy. Note reduction in FDG uptake in the aortic wall.

NIH-PA Author Manuscript

NIH-PA Author Manuscript

NIH-PA Author Manuscript

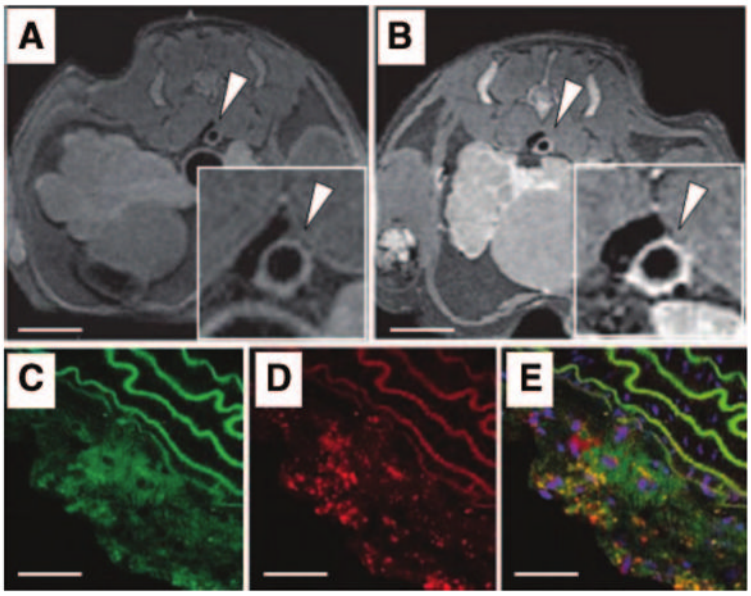

Figure 3.

Detection of macrophages with gadolinium-containing micelles targeting macrophage scavenger receptors and MRI. MR axial views of an atherosclerotic plaque in the aorta of an atherosclerotic mice before (A) and 24 hours (B) after the intravenous injection of immuno-micelles targeting the macrophage scavenger receptors (Insets are magnification of the aorta; scale bar, 1 cm). A strong enhancement was detected with MRI in the aortic wall 24 hours after injection of immuno-micelles (B; white arrowhead). Confocal fluorescence microscopy of corresponding atherosclerotic plaque demonstrated colocalization between fluorescently labeled immunomicelles (C, green color) and anti-CD68 stained macrophages (D; red stain). Areas of yellow represent overlap of labeled immunomicelles and macrophage staining on the overlaid images (E). White scale bar, 250 μm. Adapted from Amirbekian et al.[58]. Copyright © 2007 National Academy of Sciences, U.S.A.

NIH-PA Author Manuscript
NIH-PA Author Manuscript
NIH-PA Author Manuscript

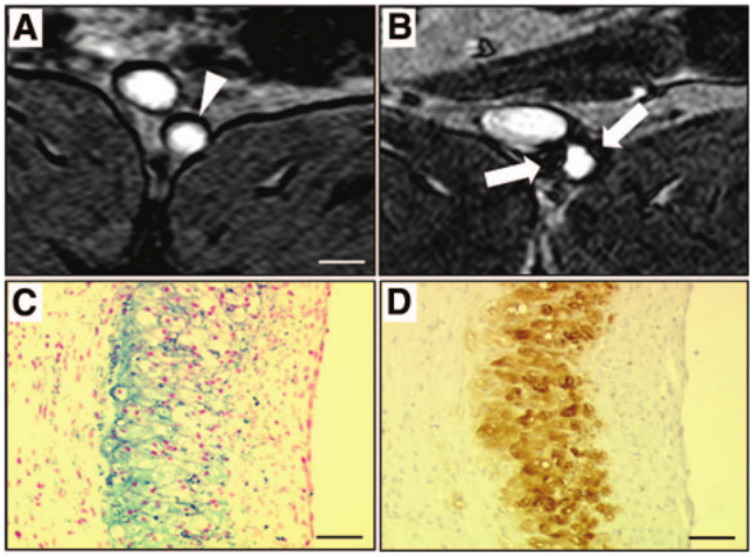

Figure 4.

Detection of macrophages with USPIO-enhanced MRI. MR axial views of an atherosclerotic plaque in a rabbit aorta before (A) and 5 days (B) after the intravenous injection of ultrasmall superparamagnetic iron oxide nanoparticles (USPIO). Five days after the intravenous injection of USPIO, strong signal voids (white arrows) were detected in the aortic wall using T2*-weighted MR sequences. Note the dark artifacts that are not related to USPIO accumulation at the fat-water interfaces. On corresponding histological section, accumulation of iron oxide nanoparticles was identified in the atherosclerotic plaque with Perls stain (C; blue staining for iron) and colocalized with macrophage infiltration detected by immunohistotochemistry using a RAM-11 monoclonal antibody for rabbit macrophages (D; brown staining). White scale bar, 5 mm; black scale bar, 30 μm.

NIH-PA Author Manuscript

NIH-PA Author Manuscript

NIH-PA Author Manuscript

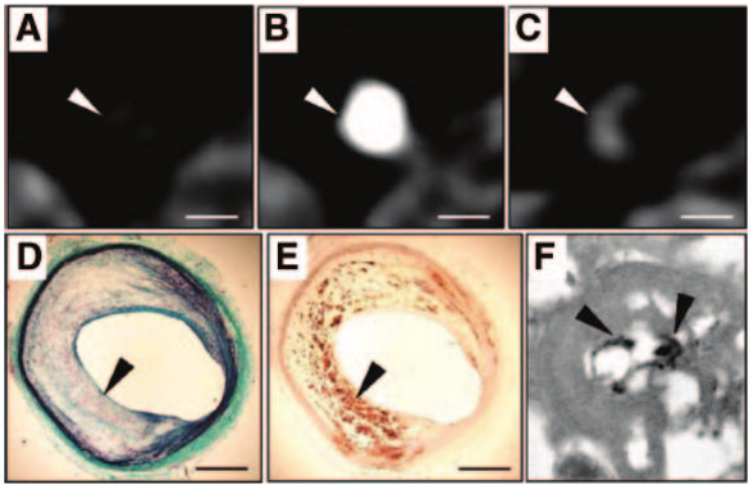

Figure 5.

Detection of macrophages with N1177-enhanced CT. CT axial views of an atherosclerotic plaque in a rabbit aorta before (A), during (B), and 2 hours after (C) the intravenous injection of the contrast agent N1177. Note the strong enhancement of the aortic wall detected with CT 2 hours after the injection of N1177 (C; white arrowhead). On axial sections corresponding to the CT images, atherosclerotic plaque was characterized by a large lipid-rich core covered by a thin cap of collagen stained in green with Masson trichrome (D; black arrowhead) and intense macrophage infiltration in the lipid-rich core detected by immunohistochemistry for macrophages with a monoclonal RAM-11 antibody (E; black arrowhead). Numerous iodine particles (black arrowheads) were detected with transmission electron microscopy, next to lipid inclusions, in lysosomes of macrophages from atherosclerotic plaques (F). White scale bar, 5 mm; black scale bar, 1 mm. Adapted from Hyafil et al.[92]